

Zolotarev Low-Pass Filter Design

G3TMG explains the filter approximation problem relating to the synthesis of Zolotarev low-pass functions with finite zeros.

This article develops a relatively simple method of using the known even-order mapping function to transform a pseudo-elliptic Chebyshev polynomial of odd order into a similarly pseudo-elliptic Zolotarev polynomial that can be used for a more efficient, realizable, low-pass, lumped element filter. “All working is shown in the method of polynomial construction for firstly, a Chebyshev response and secondly, the superior Zolotarev response, both possessing 7 poles and a single conjugate pair complexity.”

Introduction

Using a stock Chebyshev low-pass filter design, providing a well matched pass-band from dc to a pre-defined cut-off frequency ω_c , is not efficient, since more than half of the low-pass bandwidth is of no practical value. The required signal frequency to be filtered must lie above $\omega_c/2$ so as to provide any harmonic attenuation from the filters transition edge. Pseudo-elliptic filters, which use just a single conjugate pair of transmission zeros, can significantly improve harmonic rejection for the same chosen order of low-pass filtering function. This is usually achieved by adding just one more electrical component to the conventional ladder network. A much more efficient filter design can be obtained by combining the concepts that the bottom half of the passband need not to be well matched, together with the pseudo-elliptic single conjugate zeros approach.

In the 1970’s, Zolotarev functions were rediscovered and found to be more useful than the ubiquitous Chebyshev low-pass characteristic, in the context of an efficient filtering function.¹ However, the generation of the odd-ordered Zolotarev functions —

the most appropriate for low-pass filters — is very complicated and is a task that can only be described as tortuous. Interestingly, even-ordered functions are more easily obtained since they have an extremely simple closed-form solution to the mapping of existing Chebyshev reflection zeros. Although not perfect, here we describe a somewhat simpler approach to odd-ordered functions using the even-ordered solution with the addition of a simple fractional bandwidth transformation, which corrects a significant scaling error that would otherwise be introduced.

Some Basics

The transfer function for the general low-pass prototype 2-port filter is usually given in terms of the transmission scattering parameter as

$$|S_{21}(\omega)|^2 = \frac{1}{1 + \varepsilon^2 F_N^2(\omega)} \quad (1)$$

where F_N is known as the filter characteristic function of order N , and ε is a constant related to the pass-band ripple amplitude or reflection return loss R , and is defined by

$$\varepsilon = \frac{1}{\sqrt{10^{R/10} - 1}} \quad (2)$$

For the creation of a *Generalized Chebyshev* characteristic — also known as pseudo-elliptic and defined by a specified equi-ripple pass-band with arbitrarily placed stop-band transmission zeros — the filter function needs to be a rational polynomial described by

$$F_N(\omega) = \frac{P_N(\omega)}{D_N(\omega)} \quad (3)$$

It has been shown² that, in general, the denominator is given by the product of all the necessary transmission zeros such that

$$D_N(\omega) = \prod_{k=1}^N \left(1 - \frac{\omega}{\omega z_k} \right) \quad (4)$$

It should be noted here that if all the necessary zeros lie at $\omega z_k = \infty$, $D_N(\omega)=1$ and the response degenerates to the standard Chebyshev characteristic also known as an all-pole function.

There are many ways of generating the P_N polynomial,^{3,4} the simplest and most efficient being a recursion technique developed from the expansion of the Chebyshev function as shown by Amari.⁵ Therefore, having identified a preferred pass-band ripple amplitude and any required finite frequency transmission zeros, D_N and P_N can be generated and the transmission frequency response evaluated using Eq (1). Also, using energy conservation, the reflection function can also be determined because under lossless conditions

$$|S_{21}(\omega)|^2 + |S_{11}(\omega)|^2 = 1$$

so that

$$|S_{11}(\omega)|^2 = 1 - |S_{21}(\omega)|^2 \quad (5)$$

Since these response expressions are power equations they do not fully characterize the synthesized response, since phase information cannot be extracted directly, and there is no apparent means of evaluating loss or delay information. To do this we must consider the equivalent of expressing the transmission and reflection parameters in terms of voltage and/or current. Phase

information is required, of course, to form the necessary relationship between the desired responses and the electrical network that would be able to realize the target function.

This is usually achieved in the s -plane by using the complex frequency variable $s = \sigma + j\omega$ where σ represents the damping factor associated with voltage and/or current in lossy circuits and ω is the usual real frequency variable. Therefore, in synthesis we let $\sigma = 0$ so that energy conservation is obeyed and the synthesized response is ideal, or perfect. For analysis however, we can allow $\sigma > 0$, which is inversely proportional to the intended component Q 's, and represents real circuit losses. Therefore, the generated responses are imperfect and a close approximation to that which would be achieved in reality — an invaluable asset when making a determination of acceptability.

To begin then we expand Eq (1) as

$$S_{21}(s) \cdot \overline{S_{21}(s)} = \frac{1}{(1 + j\varepsilon \cdot F_N(s)) \cdot (1 - j\varepsilon \cdot F_N(s))} \quad (6)$$

Here, we can solve either or both of the denominator factors as they both contain the transmission function roots, albeit for low-pass functions in conjugate pairs. By choosing just one of the denominator factors, the phase information can be obtained directly as long as the factor is strictly *Hurwitz*, meaning that all of its roots lie in the left half of the s -plane.

We then write

$$S_{21}(s) = \frac{1}{1 + j\varepsilon \cdot F_N(s)}$$

where $s = \sigma + j\omega$

and

$$F_N(s) = \frac{P_N(s)}{D_N(s)} \quad (7)$$

then we have

$$S_{21}(s) = \frac{D_N(s)}{D_N(s) + j\varepsilon \cdot P_N(s)} \quad (8)$$

It also follows from Eq (5) that

$$S_{11}(s) = \frac{\varepsilon \cdot P_N(s)}{D_N(s) + j\varepsilon \cdot P_N(s)} \quad (9)$$

Example Generation of Generalized Chebyshev Filter Function

As an example, suppose we wish to synthesize a 7th order Chebyshev low-pass

function with a single finite frequency conjugate pair of transmission zeros at $s = \pm j 1.75$. With the five remaining zeros at infinity, Eq (4) gives the polynomial $D_7(s)$ as

$$D_7(s) = \begin{pmatrix} 1 \\ 0 \\ 0.3265 \end{pmatrix} \cdot s^r$$

$$S_{11zeros} = \begin{pmatrix} -j0.9777 \\ -j0.7988 \\ -j0.4531 \\ 0 \\ +j0.4531 \\ +j0.7988 \\ +j0.9777 \end{pmatrix} \quad (10)$$

The common denominator polynomial is therefore constructed as

$$D_7(s) + j\varepsilon P_7(s) = \begin{pmatrix} 1 \\ -0.6675 \\ 0.3265 \\ -4.995 \\ 0 \\ -9.591 \\ 0 \\ -5.330 \end{pmatrix} \cdot s^r \quad (11)$$

From Eq (8) it should also be clear that the roots of the denominator are the poles of the transmission function $S_{21}(s)$. These singularities are

$$S_{21}(poles1) = \begin{pmatrix} -0.0845 - j1.0591 \\ +0.2583 - j0.8786 \\ -0.4082 - j0.5060 \\ 0.4689 \\ -0.4082 + j0.5060 \\ +0.2583 + j0.8786 \\ -0.0845 + j1.0591 \end{pmatrix}$$

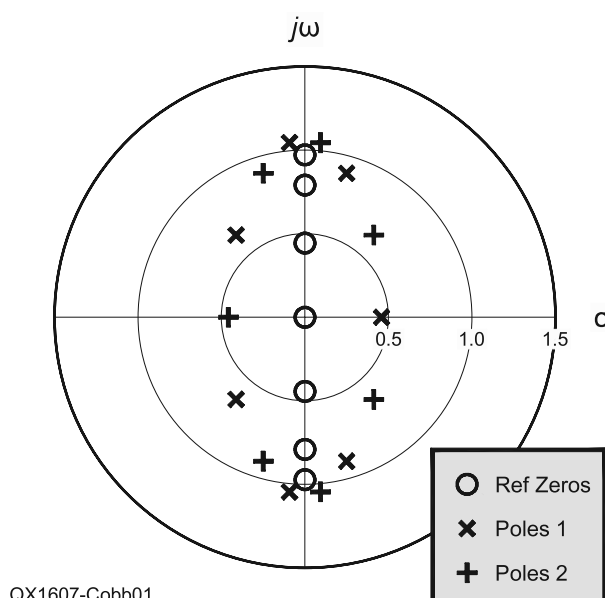


Figure 1 — The s -plane view of transmission poles and reflection zeros.

From the values shown, this polynomial is clearly not *Hurwitz* since some roots are in the left half-plane while others are in the right. However, if we had chosen the alternative denominator factor of Eq (6), the pole singularities would be the complementary ones,

$$S_{21}(\text{poles2}) = \begin{pmatrix} +0.0845 - j1.0591 \\ -0.2583 - j0.8786 \\ +0.4082 - j0.5060 \\ -0.4689 \\ +0.4082 + j0.5060 \\ -0.2583 + j0.8786 \\ +0.0845 + j1.0591 \end{pmatrix}$$

If we plot both sets of roots in the s -plane, we see in Figure 1 that the roots alternate from left to right about the $j\omega$ axis.

By just reversing the positive sign of the real part of the denominator roots, the polynomial factor will be the strictly *Hurwitz* one needed. However, after multiplying out, it will be found that the new

$$(D_N(s) + j\varepsilon \cdot P_N(s))'$$

polynomial will always be monic. It is important to note that this will affect the unity gain condition defined at each reflection zero. The new pole positions are

$$S_{21}(\text{poles}) = \begin{pmatrix} -0.0845 - j1.0591 \\ -0.2583 - j0.8786 \\ -0.4082 - j0.5060 \\ -0.4689 \\ -0.4082 + j0.5060 \\ -0.2583 + j0.8786 \\ -0.0845 + j1.0591 \end{pmatrix}$$

and are plotted in Figure 2.

Multiplying out creates the new denominator polynomial as

$$(D_7(s) + j\varepsilon \cdot P_7(s))' = \begin{pmatrix} 0.1867 \\ 0.9061 \\ 2.2076 \\ 3.6690 \\ 4.1159 \\ 3.7413 \\ 1.9708 \\ 1 \end{pmatrix} \cdot s^r$$

Because the new denominator polynomial was expected, and clearly is monic, the gain

error can be found simply by evaluating S_{21} using Eq (8) at any of the known S_{11} singularities in Eq (10) as

$$G = \left| \frac{\sum_{r=1}^7 D_r \cdot (S_{11\text{zero}})^r}{\sum_{r=1}^7 (D_r + j\varepsilon \cdot P_r) \cdot (S_{11\text{zero}})^r} \right| = 5.3303$$

G now acts as a scaling factor for all response calculations so that Eq (8) and (9) are rewritten as

$$S_{21}(s) = \frac{1}{G} \cdot \frac{D_7(s)}{(D_7(s) + j\varepsilon \cdot P_7(s))}, \quad (12)$$

and

$$S_{11}(s) = \frac{j}{G} \cdot \frac{\varepsilon \cdot P_7(s)}{(D_7(s) + j\varepsilon \cdot P_7(s))}, \quad (13)$$

Because of the unitary condition required by the scattering matrix, S_{21} and S_{11} must be, as indicated, orthogonal functions. The expression for S_{22} would be the same as Eq (13) except the j term would be $-j$.

With the polynomials thus far generated, Eq (12) and (13) produce the expected symmetrical response with the correct unity gain and phase that matches the targeted example specification. Figures 3(a) shows the overall amplitude response, Figure 3(b) shows the passband ripple, and Figure 3(c) shows phase response for 7-2 Chebyshev function.

Zolotarev Approximation

Zolotarev functions are similar to Chebyshev functions in that they have an equiripple in-band amplitude characteristic, except that with an extra design parameter x , the ripple peaks nearest to the origin are allowed to exceed the unit passband ripple amplitude. The ripple characteristics for the Zolotarev even (8th order) function are shown in Figure 4(a), and for the odd (9th order) functions in Figure 4(b), where the intervals ($x < \omega < 1$) and $(-1 < \omega < x)$ are the desired equi-ripple passbands. The Chebyshev function of the same order is also shown for comparison.

There are restrictions associated with the use of Zolotarev functions for lumped element passive circuit realizations. For example, it's not immediately obvious that even orders of Zolotarev polynomials are of little value for use in low pass filters due to the fact that the ratio of source to load resistances is usually required to be large because little of the available source power needs to be developed in the load at $\omega = 0$, or dc. They are however useful in generating dual band-pass filters where the prototype network is ultimately transformed into the real frequency band-pass domain – recently a popular area of study.

Odd ordered functions, on the other hand, do not have this problem as they always require that the source to load resistance ratio be unity. They also offer superior stopband rejection and better component values with less abrupt changes throughout the circuit when compared to similar Chebyshev pseudo-elliptic response realizations.

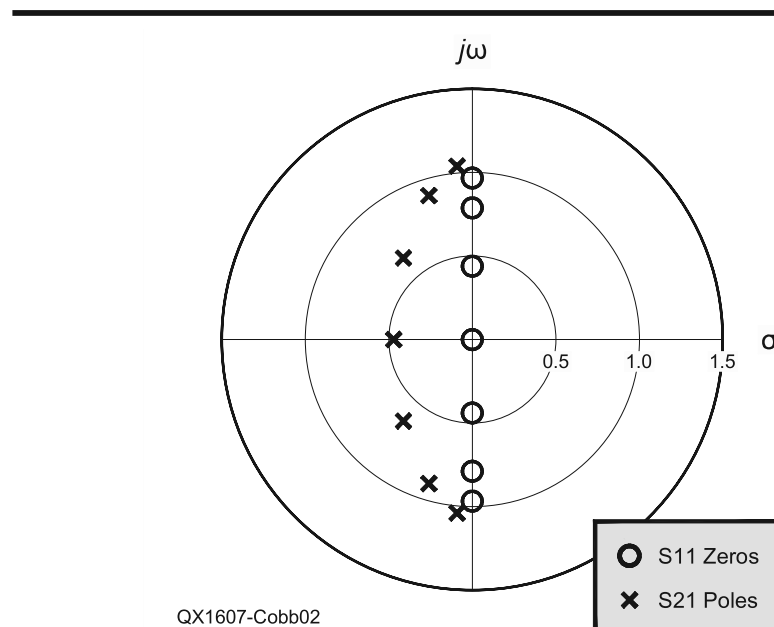
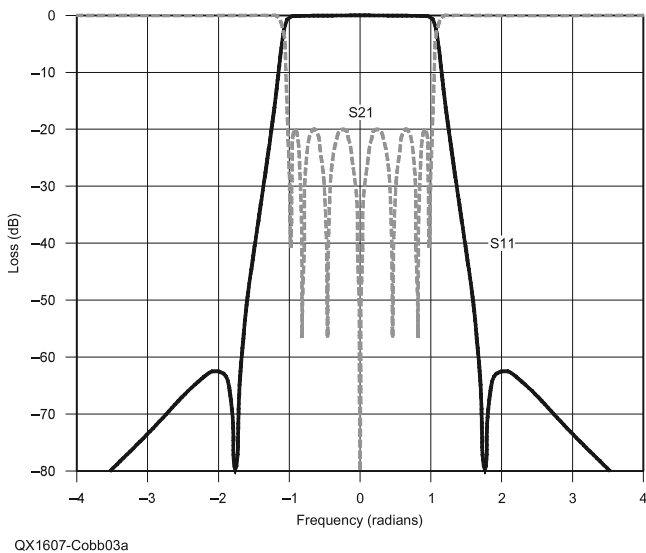
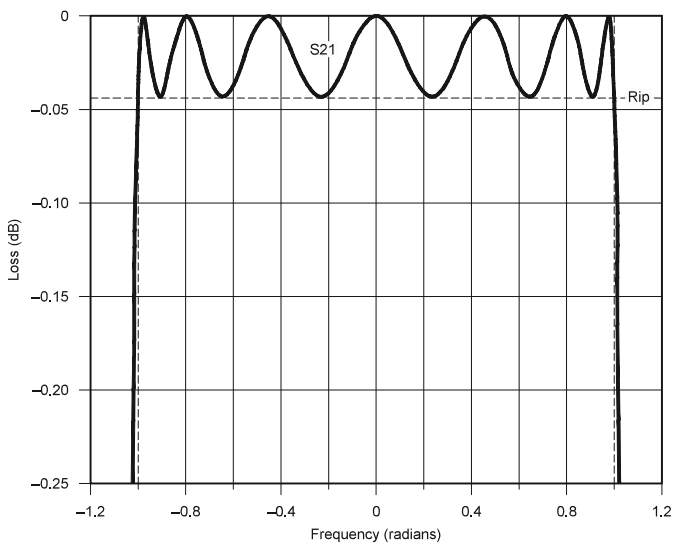


Figure 2 — The s -plane view of new transmission poles and reflection zeros.



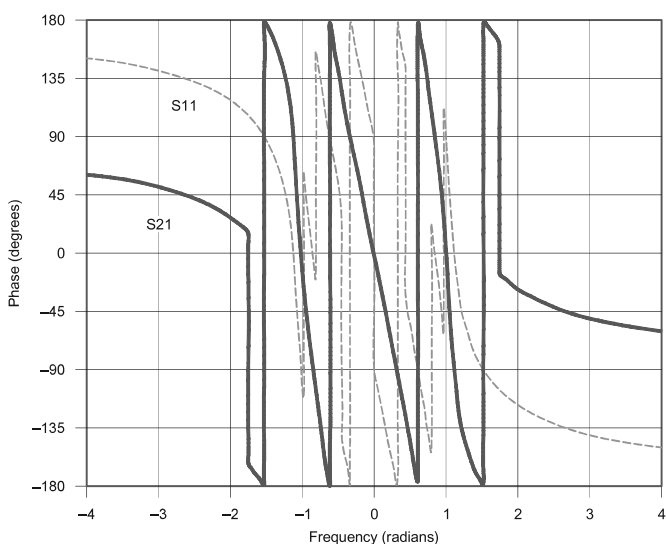
QX1607-Cobb03a

Figure 3(a) —
Overall amplitude
response for 7-2
Chebyshev function.



QX1607-Cobb03b

Figure 3(b) —
Pass-band ripple
response for
7-2 Chebyshev
function.



QX1607-Cobb03c

Figure 3(c) —
Complete phase
response for
7-2 Chebyshev
function.

Synthesis of Zolotarev Functions

Even ordered functions can easily be synthesized by transforming existing Chebyshev reflection zeros s_k into new positions s'_k using the mapping

$$s'_k = \pm\sqrt{s_k^2(1-x^2)-x^2} \quad (14)$$

where x is the real frequency value at which the equi-ripple behavior begins such that $0 < x < 1$. Note here that the equi-ripple fractional bandwidth (F_{bw}) of the new response is $(1-x)$ and when $x=0$, $F_{bw}=1$ and the original zeros are unchanged.

Unfortunately, this expression is exact only for even-ordered functions and the work of Levy and Horton^{6,7} has shown that the generation of an odd-ordered Zolotarev function that is exact is not a trivial undertaking. However, it is here shown by example, that the use of Eq (14) for odd ordered functions can yield acceptably near-Zolotarev characteristics with just one additional mapping of the x parameter so as to achieve the correct fractional bandwidth. The degree of nearness can already be seen in Figure 4(b), where the first equi-ripple turning point adjacent to, and to the right of, the positive x boundary, is slightly larger (more negative) than the -1 ideal value. Since the overall pass-band has complementary symmetry, the same deviation exists on the other side of the zero frequency axis where the first equi-ripple turning point, adjacent to, and to the left of the negative x boundary, is slightly larger (more positive) than the +1 ideal value.

Given that the highlighted pass-band amplitude errors are acceptable, it is found that the correlation between the fractional bandwidth scaling parameter x and achieved response bandwidth is the most significant issue. I decided to correct this scaling error by transforming x to a new parameter x' that equates correctly to the specified fractional bandwidth.

Consequently, I carried out a curve fitting exercise, concluding that the error characteristics are nearly linear with a small parabolic curvature. Therefore, a simple 2nd degree polynomial mapping provides correction to within 0.2% for a range of odd-ordered Zolotarev functions from 5 to 19 — a large enough range to be able to cope with most requirements. It is worth noting that filter functions below order 4 are in fact irrelevant because orders 2 and 3 are merely degenerate Chebyshev functions with parametrically scaled ripple factors.

The correction polynomial coefficients are conveniently written in matrix form such that the x to x' mapping is simply

$$x' = \begin{pmatrix} -0.5015 & 1.7150 & -0.2174 \\ -0.3164 & 1.5217 & -0.2121 \\ -0.2216 & 1.3988 & -0.1853 \\ -0.1653 & 1.3134 & -0.1555 \\ -0.1299 & 1.2566 & -0.1341 \\ -0.1062 & 1.2192 & -0.1202 \\ -0.0884 & 1.1878 & -0.1059 \\ -0.0713 & 1.1507 & -0.0838 \end{pmatrix} \cdot \begin{pmatrix} 1 \\ x \\ x^2 \end{pmatrix} \quad (15)$$

where the zero based row index is determined from $(N - 5)/2$ and N is odd from 5 to 19.

Example Generation of Generalized Zolotarev Filter Function

Suppose, for example, we wish to synthesize a 7th order Zolotarev low-pass function with a single finite frequency conjugate pair of transmission zeros at $s = \pm j 1.75$ exactly as in the previous Chebyshev case. Here, however, we wish to compress the matched region to 35% of the unit bandwidth ($F_{bw} = 0.35$) but again with the same specified ripple value.

So, the initial bandwidth scaling factor x is

$$x = 1 - F_{bw} = 0.65$$

which is corrected using Eq (15) to give

$$x' = 0.583$$

Next, the reflection zeros from Eq (10) are transformed using the mapping of Eq (14) and the new parameter x' giving

$$S_{11\text{zeros}} = \begin{pmatrix} -j0.9777 \\ -j0.7988 \\ -j0.4531 \\ 0 \\ +j0.4531 \\ +j0.7988 \\ +j0.9777 \end{pmatrix}$$

maps to $\rightarrow \begin{pmatrix} -j0.9853 \\ -j0.8724 \\ -j0.6896 \\ 0 \\ +j0.6896 \\ +j0.8724 \\ +j0.9853 \end{pmatrix} = ZS_{11\text{zeros}}$

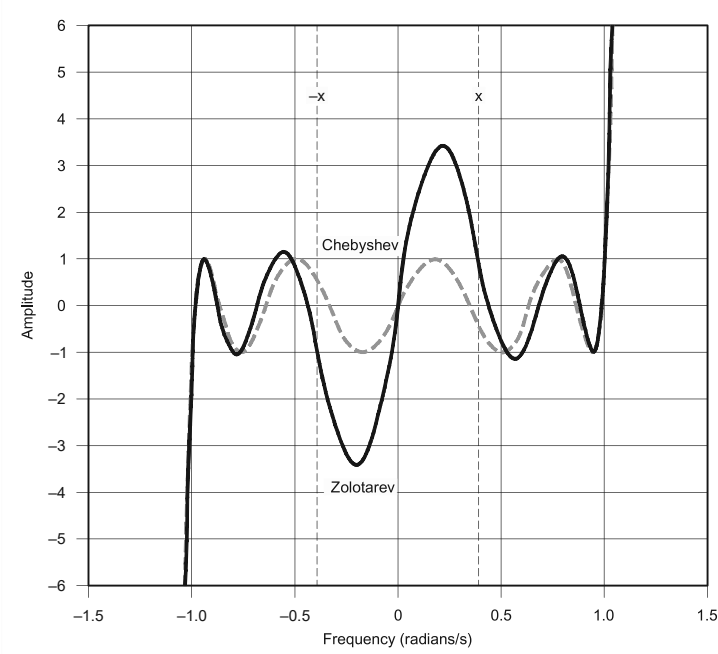
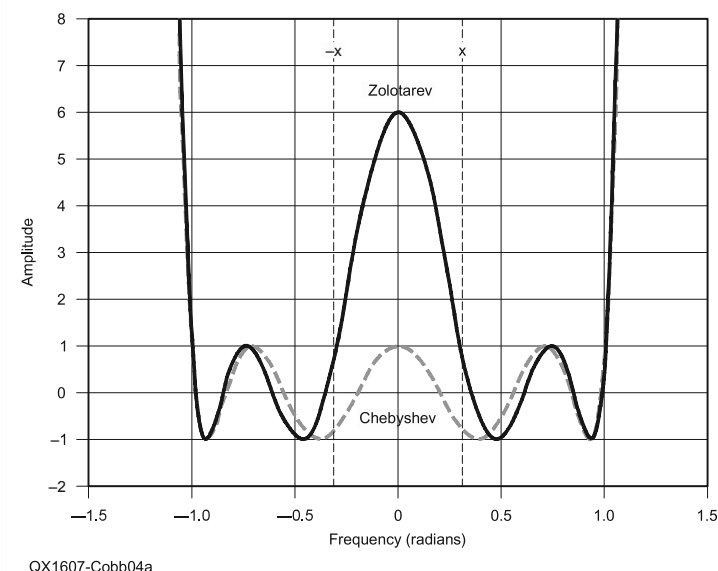
(16)

Multiplying out now gives the new P monic polynomial ZP as

$$ZP_7(s) = \begin{pmatrix} 0 \\ 0.35138 \\ 0 \\ 1.56253 \\ 0 \\ 2.20750 \\ 0 \\ 1 \end{pmatrix} \cdot s^r$$

Since we require the transmission zeros to be the same as in the previous Chebyshev case, the D_7 polynomial does not need altering and Eq (7) can be used to establish that $\lambda \cdot ZP_7(s) = P_7(s)$.

In the typical Zolotarev case, the reflection zero frequencies of either side of this expression clearly do not correspond. So, the only point where the two sides are guaranteed to be equal is at the cut-off frequency $s = \pm j$. So, evaluating at $s = j$ provides the scaling factor $\lambda = j 184.47$ so that ZP_7 is correctly specified as



$$ZP(s) = \begin{pmatrix} 64.82 \\ 288.25 \\ 407.23 \\ 184.47 \end{pmatrix} \cdot s$$

$$ZS_{21}(\text{poles}) = \begin{pmatrix} -0.05982 - j1.03886 \\ -0.16426 - j0.89974 \\ -0.17522 - j0.62451 \\ -0.14154 \\ -0.17522 + j0.62451 \\ -0.16426 + j0.89974 \\ -0.05982 + j1.03886 \end{pmatrix}$$

As in Eq (11) before, the common denominator is constructed as

$$D_7(s) + j\varepsilon ZP_7(s) = \begin{pmatrix} 1 \\ -6.515 \\ 0.3265 \\ -28.97 \\ 0 \\ -40.93 \\ 0 \\ -18.54 \end{pmatrix} \cdot s^r$$

Similarly, it will be found that the roots of this polynomial are not *Hurwitz* so the singularities are determined (they are the poles of S_{21}), and the alternating poles technique is used to reconstruct the denominator whose roots lie in the left half-plane, see Figure 5.

Multiplying out creates the new denominator polynomial

$$(D_7(s) + j\varepsilon \cdot ZP_7(s))' = \begin{pmatrix} 0.05394 \\ 0.45315 \\ 0.77662 \\ 2.07789 \\ 1.68971 \\ 2.64942 \\ 0.94013 \\ 1 \end{pmatrix} \cdot s^r$$

As before, this new denominator polynomial is monic and the gain error needs to be found by evaluating S_{21} using Eq (8) at any of the known ZS_{11} singularities from Eq (16).

$$GZ = \left| \frac{\sum_{r=1}^7 D_r \cdot (ZS_{11\text{zero}})^r}{\sum_{r=1}^7 (D_r + j\varepsilon \cdot PZ_r)' \cdot (ZS_{11\text{zero}})^r} \right| = 18.540$$

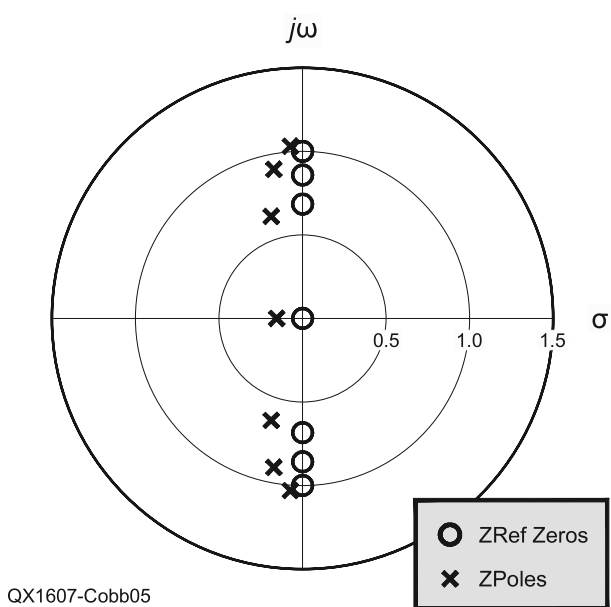


Figure 5 — The s -plane view of Zolotarev transmission poles and reflection zeros.

With the new

$$(D_7(s) + j\varepsilon \cdot P_7(s))'$$

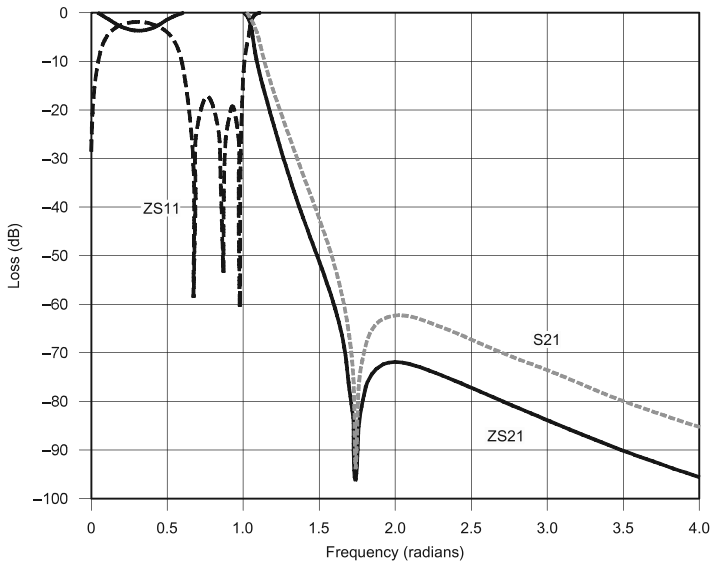
polynomial and GZ , Eq (12) and (13) are used to produce the expected symmetrical response with the correct unity gain and phase that matches the desired example specification. Figures 6(a) shows the overall amplitude response, Figure 6(b) shows the pass-band ripple and Figure 6(c) shows the complete phase response for 7-2 Zolotarev function. Here, only the positive real frequencies of the analyzed response are shown for relevance to a real low-pass frequency response demonstrating the near Zolotarev behavior in terms of both the pass-band ripple amplitude and superior rejection, when compared to the equivalent Chebyshev response, which is also shown. Finally, observe that using the new transformation Eq (15), the equi-ripple fraction bandwidth achieved is precisely 0.35 of the unit bandwidth, as was intended.

Concluding Remarks

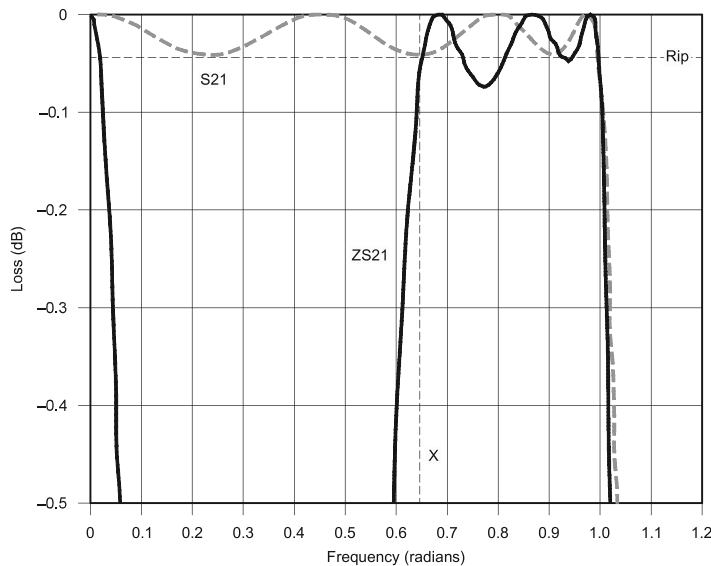
A technique used to create the necessary transmission and reflection polynomials approximating the superior Zolotarev low-pass filter function of odd order has been shown. A transformation Eq (15) has also been shown to be effective in correcting the scaling parameter x so that the simple reflection zero position mapping function Eq (14) can be systematically applied in a predetermined synthesis procedure.

The only disadvantage of using such a simple procedure is the slight distortion that occurs in the target equi-ripple behavior for the first ripple most adjacent to, and on the right side of, the low frequency cut-off point of the required passband. However, it can be shown that after component extraction, the degree of observed distortion is comparable with the SVC (standard value component) design tolerance issue. If an optimization technique is adopted, as demonstrated by Gary Appel⁸, it is suggested that using the synthesis procedure shown here provides a better and more stable starting point yielding the least number of iterations to achieve precise results. In practice, the response can easily be corrected by hand in the circuit simulation tuning environment for responses up to the maximum order of 19 proposed here, well beyond typical design requirements.

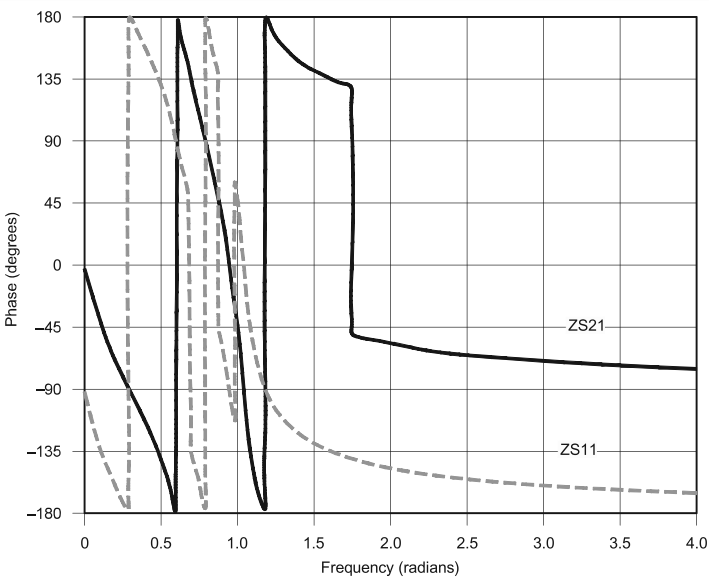
To demonstrate the practical use of this synthesis procedure, a second article will follow, which shows several examples of real filters constructed using two different inductor techniques. These are air-cored shielded solenoid and ferrite toroidal inductors appropriate for VHF and HF designs respectively.



QX1607-Cobb06a



QX1607-Cobb06b



QX1607-Cobb06c

Figure 6(a)
— Overall
amplitude
response for
7-2 Zolotarev
function.

Gary Cobb, G3TMG, has held the same call sign since he was first licensed in 1964. He holds a BA in Mathematics, an MSc in Microwave Physics, and is a Life Member of the IEEE. His early professional career development took place in the defense industry where he designed high resolution microwave antenna interferometry systems. His later, research activities moved toward the realization of adaptive arrays for ship-borne radio communications in a Navy environment. Gary spent the last 20 years in military and commercial satellite payload engineering, developing output multiplexers, multi-port amplifiers and filter techniques appropriate for high-power geostationary systems. Now retired, Gary operates CW and SSB on HF and VHF amateur bands with a special interest in sporadic-E during the summer months.

Notes

¹R. Levy, "Generalized Rational Function Approximation in Finite Intervals Using Zolotarev Functions", *IEEE Trans, MTT*, Vol 18, December, 1970, pp 1051-1064.

²R.J. Cameron "Fast generation of Chebyshev filter prototypes with asymmetrically-pre-scribed transmission zeros", *ESA Journal*, Vol 6, 1982, pp 83-95.

³R.J. Cameron et al, *Microwave Filters for Communications Systems*, John Wiley & Sons Inc, 2007, Chapter 6.3.

⁴J.D. Rhodes and S.A. Alseyab, "The generalized Chebyshev low-pass prototype filter", *Circuit Theory Application*, Vol 8, 1980, pp 113-125.

⁵S. Amari, "Synthesis of Cross-Coupled Resonator Filters Using an Analytical Gradient-Based Optimization Technique", *IEEE MTT*, Vol 48, Sep, 2000, pp 1559-1564.

⁶M.C. Horton, "Quasi-Lowpass, Quasi-Elliptic Symmetric Filter", *IEEE Trans, MTT-S Digest*, 1987, pp 129-132.

⁷See Note 1.

⁸Gary Appel, "Filter Synthesis using Equal Ripple Optimization", *QEX*, Jul/Aug, 2011, pp 22-30.

Figure 6(b)
— Pass-band
ripple response
for 7-2 Zolotarev
function.